

Quantum transport and localization in biased periodic structures under bi- and polychromatic driving

A Klumpp*, D Witthaut, and H J Korsch
FB Physik, Technische Universität Kaiserslautern
D-67653 Kaiserslautern, Germany

November 12, 2018

Abstract

We consider the dynamics of a quantum particle in a one-dimensional periodic potential (lattice) under the action of a static and time-periodic field. The analysis is based on a nearest-neighbor tight-binding model which allows a convenient closed form description of the transport properties in terms of generalized Bessel functions. The case of bichromatic driving is analyzed in detail and the intricate transport and localization phenomena depending on the communicability of the two excitation frequencies and the Bloch frequency are discussed. The case of polychromatic driving is also discussed, in particular for flipped static fields, i.e. rectangular pulses, which can support an almost dispersionless transport with a velocity independent of the field amplitude.

1 Introduction

Quantum transport properties in periodic structures (lattices) are highly non-intuitive, in particular in view of their localization properties (see, e.g., [1]). Classically, a particle in a periodic potential is localized in a single well at low energies, whereas a quantum system shows the well known Bloch band/gap structure with transporting bands. If a constant field F_0 is added, the quantum states in a band with width G become localized to an interval G/F_0 ,

*Present address: Institut für Physik, Universität Kassel, D-34109 Kassel, Germany

contrary to our intuition. In this region, the wave functions show the celebrated Bloch oscillations [2] with the Bloch frequency $\omega_B = F_0 d / \hbar$, where d is the period of the potential, and there is no directed transport. This localization is, of course, approximate because of the decay to infinity by Zener tunneling [3], an effect of longer time scales at least for weak fields. An additional time-periodic driving $F(t)$ re-introduces the quantum transport which can be suppressed again for special choice of the parameters. In the following we will neglect the decay and confine ourselves to the minimal model system, the single-band tight-binding hamiltonian with nearest-neighbor coupling

$$\hat{H} = -\frac{G}{4} \sum_{\ell=-\infty}^{+\infty} (|\ell\rangle\langle\ell+1| + |\ell+1\rangle\langle\ell|) + dF \sum_{\ell=-\infty}^{+\infty} \ell|\ell\rangle\langle\ell|, \quad (1)$$

where $|\ell\rangle$ are the Wannier states which are exponentially localized in the ℓ -th potential well and G is the width of the Bloch band for $F = 0$. Let us recall that for a static field $F = F_0$ the extension of the Bloch oscillation is approximately

$$L = G/F_0 \quad (2)$$

as easily deduced from the tilted band picture.

For the best understood case of a monochromatic driving $F(t) = F_0 - F_1 \cos(\omega_1 t)$ where the driving frequency is in resonance with the Bloch frequency, $\omega_B = n\omega_1$, $n = 1, 2, \dots$, a suppression of transport, denoted as a *dynamic localization* is found if the condition

$$J_n(dF_1/\hbar\omega_1) = 0 \quad (3)$$

is satisfied [1, 4, 5], where $J_n(z)$ is the (ordinary) Bessel function. Otherwise transport with a velocity proportional to $J_n(dF_1/\hbar\omega)$ is found.

For the general case of a bi- or polychromatic periodic driving the particle dynamics is found to be quite complicated and unexpected effects have been observed. These effects may be used to manipulate the quantum dynamics. The aim of the present study is to investigate the transport and localization properties for a bi-chromatic driving extending previous studies by Liu and Zhu [6], Suqing *et al.* [7] and Yashima *et al.* [8]. In addition, we will briefly consider the even less explored realm of polychromatic driving

We base our analysis on a Lie-algebraic approach introduced by one of the authors [9] (see also [10] for an extension to two space dimensions). Following Ref. [9], we introduce the abbreviations $f_t = dF(t)/\hbar$ and $g = -G/4\hbar$ which may also depend on time in general. Then the Hamiltonian can be conveniently expressed in terms of the hermitian position operator

$\hat{N} = \sum_{\ell} \ell |\ell\rangle\langle\ell|$ and the unitary shift operator $\hat{K} = \sum_{\ell} |\ell\rangle\langle\ell+1|$:

$$\frac{1}{\hbar} \hat{H} = g (\hat{K} + \hat{K}^\dagger) + f_t \hat{N}. \quad (4)$$

The dynamics of expectation values depends on the initial state

$$|\psi(t=0)\rangle = \sum_{\ell} c_{\ell} |\ell\rangle \quad (5)$$

characterized by the coherence parameters

$$K = \sum_{\ell} c_{\ell-1}^* c_{\ell} = |K| e^{i\kappa} \quad (6)$$

$$L = \sum_{\ell} c_{\ell-2}^* c_{\ell} = |L| e^{i\nu} \quad (7)$$

$$J = \sum_{\ell} (2\ell - 1) c_{\ell-1}^* c_{\ell} = |J| e^{i\mu}. \quad (8)$$

In the following we will assume a symmetric normalized Gaussian state $c_{\ell} \sim e^{-\ell^2/4\sigma^2}$ which allows for a broad initial distribution ($\sigma \gg 1$) an approximate evaluation of the coherence parameters by replacing sums by integrals:

$$K \approx e^{-1/8\sigma^2}, \quad L \approx e^{-1/2\sigma^2}, \quad J \approx 0. \quad (9)$$

The time evolution operator can be written as a product of exponentials [9]

$$\hat{U}(t) = e^{-i\eta_t \hat{N}} e^{-i\chi_t \hat{K}} e^{-i\chi_t^* \hat{K}^\dagger}, \quad (10)$$

with

$$\eta_t = \int_0^t f_{\tau} d\tau \quad \text{and} \quad \chi_t = g \int_0^t e^{-i\eta_{\tau}} d\tau = |\chi_t| e^{-i\phi_t}. \quad (11)$$

An advantage of the product form (10) is the simple evaluation of matrix elements and expectation values, as for instance the mean value of the position \hat{N} ,

$$\langle \hat{N} \rangle_t = \langle \hat{N} \rangle_0 + i (\chi_t \langle \hat{K} \rangle_0 - \chi_t^* \langle \hat{K}^\dagger \rangle_0) = \langle \hat{N} \rangle_0 + 2|K| |\chi_t| \sin(\phi_t - \kappa) \quad (12)$$

with the coherence parameter $K = |K| e^{i\kappa}$ specified in (6). For a symmetric initial state we have $\kappa = 0$ and an elementary calculation provides an upper bound of the mean transport velocity

$$v_{\text{trans}} = \frac{\langle \hat{N} \rangle_t - \langle \hat{N} \rangle_0}{t} \leq 2|gK|. \quad (13)$$

The time evolution of the width of the wave packet is given by [9]

$$\begin{aligned}\Delta_N^2(t) = & \Delta_N^2(0) + 2|\chi_t|^2 \{1 - |L| \cos(2\phi_t - \nu) - 2|K|^2 \sin^2(\phi_t - \kappa)\} \\ & + 2|\chi_t| \{2\langle N \rangle_0 |K| \sin(2\phi_t - \kappa) + |J| \sin^2(\phi_t - \mu)\}.\end{aligned}\quad (14)$$

which simplifies to

$$\Delta_N^2(t) = \Delta_N^2(0) + 2|\chi_t|^2 \{1 - |L| \cos(2\phi_t) - 2|K|^2 \sin^2(\phi_t)\} \quad (15)$$

for a real symmetric Gaussian initial wave packet. With $|K| = e^{-1/8\sigma^2}$ and $|L| = e^{-1/2\sigma^2}$ the dispersion depends on σ as $\Delta_N^2(t) - \Delta_N^2(0) \sim 1/\sigma^2$ for large values of σ . This leading order term can, however, be suppressed at times t for which the function χ_t is purely imaginary, i.e. $\cos(2\phi_t) = -1$ and $\sin^2(\phi_t) = 1$. One can easily show that this implies

$$\Delta_N^2(t) - \Delta_N^2(0) = |\chi_t|^2 \frac{1}{4\sigma^4} + O(\sigma^{-6}) \quad (16)$$

and the dispersion is strongly reduced at these times. This condition will be satisfied for the example of the shuttling transport discussed below in section 5.1.

2 Time periodic driving

In the following, we will assume a time-independent nearest-neighbor coupling $g = g > 0$ and a periodic driving term

$$f_t = f_0 + \tilde{f}_t, \quad \tilde{f}_{t+T} = \tilde{f}_t, \quad (17)$$

where $f_0 \leq 0$ is constant and \tilde{f}_t vanishes on the average. This implies a Bloch frequency $\omega_B = f_0$.

It can easily be shown by Fourier expansion that both functions in (11) can be separated into a linear growing and a periodically oscillating part (cf. [9]):

$$\eta_t = f_0 t + \tilde{\eta}_t, \quad \chi_t = \gamma t/2 + \tilde{\chi}_t \quad (18)$$

where γ is different from zero if the driving period T is in resonance with the Bloch period $T_B = 2\pi/\omega_B$,

$$T = n T_B, \quad n \in \mathbb{N}. \quad (19)$$

The coefficient γ controlling the transport properties is given by

$$\gamma = \frac{2\chi_T}{T} = \frac{2g}{T} \int_0^T e^{-in\omega t - i\tilde{\eta}_t} dt \quad (20)$$

with $\omega = 2\pi/T$. At time T the time evolution operator (10) commutes with \hat{K} and the simultaneous eigenstates of \hat{K} and $\hat{U}(T)$ have eigenvalues $e^{i\kappa d}$ and $e^{-i\epsilon T}$, respectively, where the quasienergy ϵ depends on the quasimomentum κ as

$$\epsilon(\kappa) = |\gamma| \cos(\kappa d + \arg(\gamma)) \quad (21)$$

denoted as the (quasi)dispersion relation. It may be of interest to realize that the possible values of γ are bounded by the width of the dispersion relation for the non-biased system

$$|\gamma| \leq 2|g|, \quad (22)$$

a well known property of Fourier integrals.

The mean value of the wave packet moves with an average velocity

$$\begin{aligned} V_{\text{trans}} &= \frac{\langle \hat{N} \rangle_{Td}}{T} = v_{\text{trans}} d \\ v_{\text{trans}} &= \frac{i}{T} \left(\chi_T \langle \hat{K} \rangle_0 - \chi_T^* \langle \hat{K}^\dagger \rangle_0 \right) = -|\gamma| \sin(\kappa d + \arg(\gamma)), \end{aligned} \quad (23)$$

where the initial condition is written as $\langle \hat{K} \rangle_0 = e^{i\kappa d}$. As expected, this mean velocity can also be expressed as $v_{\text{trans}} = d\epsilon/d\kappa|_\kappa$. Note that v_{trans} is bounded from above

$$v_{\text{trans}} \leq |\gamma| \leq 2|g| \text{ or } V_{\text{trans}} \leq 2d|g|. \quad (24)$$

If the system parameters are adjusted such that $\gamma = 0$, the band (21) collapses and the non-oscillatory term in χ_T vanishes with the consequence that there is no transport, i.e. we have dynamic localization.

3 Bichromatic driving

Let us consider a combined dc- and bichromatic ac-driving

$$f_t = f_0 - f_1 \cos(\omega_1 t) - f_2 \cos(\omega_2 t + \delta) \quad (25)$$

with a phase shift δ . Note that this function is aperiodic for incommensurable frequencies ω_1 and ω_2 , which is not necessarily true for a sum of two arbitrary periodic functions with incommensurable periods; an example can be found in [11]. For commensurable frequencies f_t is periodic.

With $f_0 = \omega_B$ and $u = f_1/\omega_1$, $v = f_2/\omega_2$ we obtain

$$\eta_t = \int_0^t f_\tau d\tau = \omega_B t - u \sin(\omega_1 t) - v \sin(\omega_2 t + \delta). \quad (26)$$

The function χ_t in eq. (11) which determines the dynamics can be expressed in terms of Bessel functions using the generating function

$$e^{ix \sin z} = \sum_{\mu=-\infty}^{\infty} J_{\mu}(x) e^{i\mu z}. \quad (27)$$

With the abbreviation $\omega_{\mu,\nu} = \omega_B - \mu\omega_1 - \nu\omega_2$ this yields

$$\begin{aligned} \chi_t &= \int_0^t g e^{-i\eta\tau} d\tau = g \int_0^t e^{-i(\omega_B t - u \sin(\omega_1 t) - v \sin(\omega_2 t + \delta))} d\tau \\ &= g \sum_{\mu=-\infty}^{\infty} \sum_{\nu=-\infty}^{\infty} J_{\mu}(u) J_{\nu}(v) e^{i\nu\delta} \int_0^t d\tau e^{-i\omega_{\mu,\nu}\tau}. \end{aligned} \quad (28)$$

The remaining integration is elementary, however one has to distinguish the cases of resonant and non-resonant driving.

In the resonant case, we have

$$\omega_B = \mu\omega_1 + \nu\omega_2 \quad (29)$$

for certain integers μ, ν . Let us denote the set of all indices μ, ν satisfying (29) by \mathbb{B} . We then have

$$\chi_t = \gamma t/2 + 2g \sum_{(\mu,\nu) \notin \mathbb{B}} J_{\mu}(u) J_{\nu}(v) e^{i\nu\delta} \frac{1}{\omega_{\mu,\nu}} e^{-i\omega_{\mu,\nu}t/2} \sin \frac{\omega_{\mu,\nu}t}{2}, \quad (30)$$

with

$$\gamma = \frac{2\chi_T}{T} = 2g \sum_{(\mu,\nu) \in \mathbb{B}} J_{\mu}(u) J_{\nu}(v) e^{i\nu\delta}. \quad (31)$$

If $\mathbb{B} \neq \emptyset$ the first term in (30) is growing linearly in time and thus dominating the long time dynamics. In this case we can observe transport.

It is instructive to have a brief look at the monochromatic driving first. This case is recovered for $v = 0$, observing $J_{\nu}(0) = \delta_{\nu,0}$ and hence

$$\chi_t = \gamma t/2 + 2g \sum_{\mu \notin \mathbb{B}} J_{\mu}(u) \frac{1}{\omega_{\mu}} e^{-i\omega_{\mu}t/2} \sin \frac{\omega_{\mu}t}{2}, \quad (32)$$

with $\omega_{\mu} = \omega_B - \mu\omega_1$ (cf. [1,9]) If the resonance condition $\omega_B = \mu\omega_1$ is satisfied, we have

$$\gamma = 2g J_{\mu}(u) \quad (33)$$

and therefore an average transport with velocity proportional to the Bessel function $J_\mu(u) = J_\mu(f_1/\omega_1)$. This linear transport is superimposed by an oscillating part, which is periodic with the Bloch period T_B for resonant driving. By adjusting the value of the driving amplitude f_1 one can change the direction of the transport or bring it to a standstill for $J_\mu(f_1/\omega_1) = 0$, the dynamic localization.

For bichromatic driving, the situation is more complicated. We distinguish two cases:

Incommensurable driving frequencies ω_1 and ω_2 :

If the ratio ω_2/ω_1 is irrational, the resonance condition (29) leads to $\omega_B/\omega_1 = \mu + \nu\omega_2/\omega_1$. This can only be satisfied for a special irrational value of the ratio ω_B/ω_1 , for example by an appropriate dc-field F_0 . These cases are of measure zero and *typically* there is *no transport*. If, however, the system parameters are tuned to special values satisfying the resonance condition (29), then there exists only a single pair $(\mu, \nu) \in \mathbb{B}$ as can be easily checked and we have transport with velocity

$$\gamma = 2gJ_\mu(u)J_\nu(v) e^{i\nu\delta}. \quad (34)$$

Commensurable driving frequencies ω_1 and ω_2 :

If $\omega_2/\omega_1 = q/p$ for integers q and p with no common divisor and if the resonance condition (29) is satisfied for a particular pair (M, N) one can find all solutions by $(\mu, \nu) = (M - qk, N + pk)$ with $k \in \mathbb{Z}$, i.e.

$$\mathbb{B} = \{(M - qk, N + pk), k \in \mathbb{Z}\}. \quad (35)$$

This can be shown as follows: The resonance condition (29) can be rewritten as the Diophantine equation

$$n = p\mu + q\nu \quad \text{with} \quad n = p\omega_B/\omega_1 \in \mathbb{Z}. \quad (36)$$

A solution $(\mu, \nu) = (M, N)$ of this equation always exists if p and q have no common divisor and can be found systematically by, e.g., the Euclid algorithm [12]. We therefore have an infinite number of solutions. Note that the choice of the special solution (M, N) is arbitrary. For rational frequency ratios the function (31) is determined by three integers, p , q , n , and we can express it in the convenient form

$$\gamma = 2g e^{iN\delta} J_n^{p,q}(u, v; e^{ip\delta}) \quad (37)$$

in terms of the two-dimensional, one-parameter Bessel function

$$J_n^{p,q}(u, v; z) = \sum_{k=-\infty}^{\infty} J_{M-qk}(u) J_{N+pk}(v) z^k \quad (38)$$

	ω_B/ω_1 irrational	ω_B/ω_1 rational
ω_2/ω_1 irrational	localization (transport possible)	localization
ω_2/ω_1 rational	localization	transport (localization possible)

Table 1: Transport properties for a bichromatically driven biased lattice with Bloch frequency ω_B .

where (M, N) is an arbitrary solution of the Diophantine equation (36). An introduction into the properties of two-dimensional Bessel functions can be found in [13].

The two-dimensional generalized Bessel functions (38) satisfy the inequality $|J_n^{p,q}(u, v; z)| \leq 1/\sqrt{2}$ for $n \neq 0$. This implies that the maximum transport velocity

$$v_{\text{trans,max}} = |\gamma| = 2|g| |J_n^{p,q}(u, v; e^{ip\delta})| \quad (39)$$

is bounded as $|\gamma| \leq \sqrt{2}g < 2g$.

For commensurable driving frequencies ω_1 and ω_2 , $\omega_2/\omega_1 = q/p$, and driving amplitudes f_1, f_2 we have the following behavior:

If the ratio ω_B/ω_1 is irrational, the condition (29) cannot be satisfied and we have no transport.

If ω_B/ω_1 is rational with $n = p\omega_B/\omega_1$ we typically have transport with transport velocity proportional to $J_n^{p,q}(f_1/\omega_1, f_2/\omega_2)$. This transport can, however, be stopped for special values of the system parameters and dynamic localization is observed. It should be noted that this case is always met for pure ac-driving ($\omega_B = 0$).

The transport and localization properties of a bichromatically driven system are summarized in Table 1. The following section considers some exemplary cases in more detail.

4 Case studies for resonant driving

In this section, we will discuss the transport and localization properties in some more detail for the most interesting case of resonant driving $\omega_B = \mu\omega_1 + \nu\omega_2$. The driving frequencies are assumed to be commensurable, $\omega_2/\omega_1 = p/q$

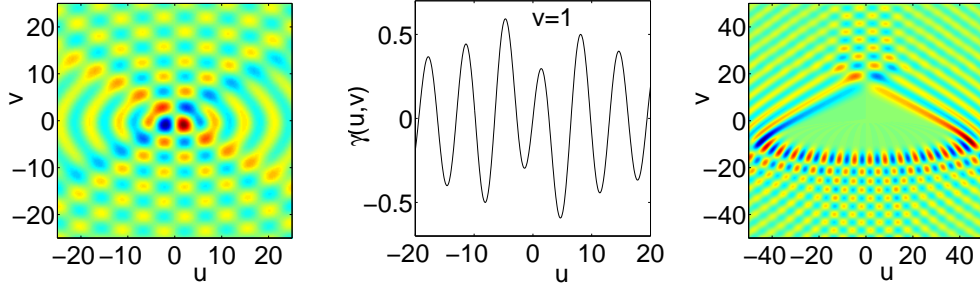


Figure 1: Transport coefficient γ as a function of the parameters $u = f_1/\omega_1$ and $v = f_2/\omega_2$ for a bichromatic driving with $\omega_2 = 2\omega_1$ at resonance with the Bloch frequency ω_B , i.e. $\omega_1 + \omega_2 = n\omega_B$. Shown are examples for $n = 1$ (left and middle) and $n = 29$ (right), where the figure in the middle shows γ for a fixed parameter $v = 1$.

with coprime integers p and q , where, w.l.o.g., we can choose p as the smaller one of these numbers. Let us recall that the ac-driving period T is equal to an integer number of Bloch periods, $T = nT_B$, where n can be expressed as $n = pM + qN$ with integer $(M, N) \in \mathbb{B}$. We will also assume that the force term is symmetric in time, $f(-t) = f(t)$, i.e. the phase shift δ in (25) is equal to zero, with the consequence that the two-dimensional one-parameter Bessel functions reduce to simple two-dimensional ones [13]. The transport properties of the system are then determined by the parameter

$$\gamma = 2g J_n^{p,q}(u, v). \quad (40)$$

with variables $u = f_1/\omega_1$ and $v = f_2/\omega_2$. In this case γ is real and its sign, the sign of the Bessel function, directly gives the direction of transport. Here we are in particular interested in the parameter values leading to dynamic localization. These values are given by the zeros of $J_n^{p,q}(u, v)$, i.e. the nodal lines of the two-dimensional Bessel function.

In previous studies the special case of the bichromatic driving with $\omega_2 = 2\omega_1$ attracted most attention and we will start with this special case in the following. For simplicity we fix $g = 1$ and $\omega_1 = 1$. The resonance condition for the static field (36) then reads $n = \omega_B/\omega_1 = f_0/\omega_1$. In our first examples we fix the amplitude of one driving as $f_2 = \omega_2$, i.e $v = 1$, and consider the case $\omega_B = \omega_1$, i.e. $n = 1$. The transport coefficient given by $\gamma = 2J_1^{1,2}(u, v)$ is shown in figure 1 in dependence of u and v (left-hand side) and for $v = 1$ fixed (middle). Numerically we find a global maximum at $u = -4.68$ and a nodal line at $u = -6.49$ for $v = 1$.

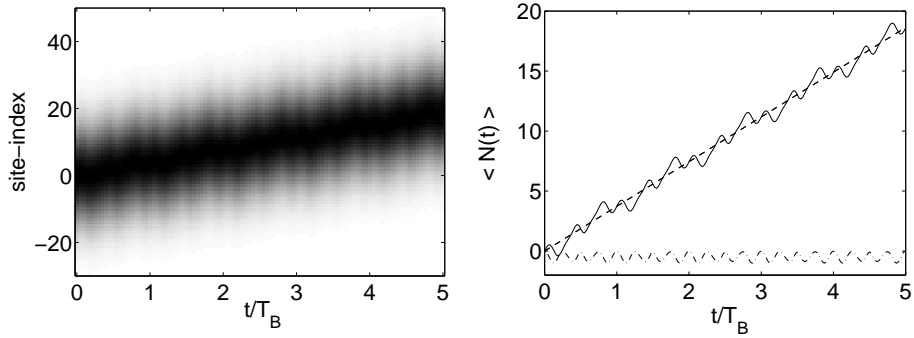


Figure 2: Left: Dynamics of a gaussian wave packet with initial momentum $\kappa_0 = -\pi/2$ for a bichromatic driving with amplitudes $v = 1$ and $u = -4.68$ in a greyscale plot. Right: Position expectation value $\langle \hat{N}(t) \rangle$ for $\kappa_0 = -\pi/2$ (solid line) and $\kappa_0 = 0$ (dash-dotted line) in comparison with the transport coefficient γt (dashed line).

We consider the time evolution of a broad Gaussian wavepacket

$$|\psi(t=0)\rangle \sim \sum_{\ell} \exp\left(-\ell^2/(2\sigma)^2 + i\kappa_0\ell\right) |\ell\rangle \quad (41)$$

with $\sigma = 10$. For such a broad gaussian wavepacket the coherence parameter K is given by $|K| \approx 1$ and $\kappa \approx \kappa_0$. The left-hand side of figure 2 shows the dynamics of such a wave packet for $\kappa_0 = -\pi/2$, which is rapidly transported. The right-hand side shows the expectation values $\langle \hat{N}(t) \rangle$ of the position for $\kappa_0 = 0$ and $\kappa_0 = -\pi/2$. The transport coefficient γt is shown as a dashed line for comparison. The sine in equation (12) is approximately one for $\kappa_0 = -\pi/2$ such that the fastest possible transport is observed which is given by γt . For $\kappa_0 = 0$ the sine in equation (12) is approximately zero so that the wavepacket stays at rest. However, this localization is only due to the special initial state chosen in this example. Depending on the value of κ_0 , the wavepacket will be transported with a velocity in the interval $[-\gamma, \gamma]$. Localization, i.e. $v_{\text{trans}} = 0$ is only found for $\kappa_0 = 0$.

The situation is different for $u = -6.49$, for which $J_1^{1,2}(u, v) = 0$, i.e. dynamical localization is found. Now *every* wavepacket will be localized regardless of its initial momentum κ . This is illustrated in figure 3 on the left where the position expectation value $\langle \hat{N}(t) \rangle$ is shown for $\kappa_0 = 0$ and $\kappa_0 = -\pi/2$. The right hand side of figure 3 shows the time evolution of the width of the wavepacket with $\kappa_0 = 0$ for $u = -4.68$ (transport) and $u = -6.49$ (dynamical localization). As the dispersion is also governed by the function $|\chi_t|$, no broadening is observed in the case of dynamical localization.

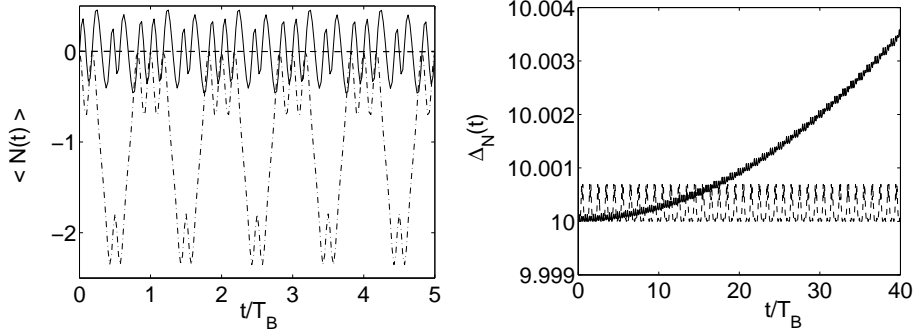


Figure 3: Left: Dynamical Localization. For $u = -6.49$ any wave packet is localized around $n = 0$ regardless of the initial momentum. The evolution of the position expectation $\langle \hat{N}(t) \rangle$ is shown for $\kappa_0 = -\pi/2$ (solid line) and $\kappa_0 = 0$ (dash-dotted line). Right: Dispersion of a gaussian wave packet with $\kappa_0 = -\pi/2$ for $u = -4.68$ (transport, solid line) and $u = -6.49$ (dynamical localization, dashed).

Next we consider an example, where the field amplitudes are large in comparison to the driving frequencies. Then $n = f_0/\omega \ll 1$ as well as $u, v \ll 1$ and asymptotic approximations for the relevant Bessel functions are available [13]. In fact we consider a driving amplitude $v = -20$ and a static field strength with $n = 29$. Dynamical localization is observed if the driving amplitudes u is chosen such that $J_2^{1,2}9(u, v) = 0$. Explicit estimates for these values are derived from the asymptotic approximations of this Bessel function. For $n < 2|v|$ one finds

$$u \sqrt{\frac{1}{2} - \frac{n}{4v}} = \begin{cases} (2j+1)\frac{\pi}{2} & n \text{ even} \\ j\pi & n \text{ odd} \end{cases} \quad , \quad j = 0, \pm 1, \pm 2, \dots \quad (42)$$

and for $n > 2|v|$ with $v < 0$

$$u \sqrt{\frac{1}{2} - \frac{n}{4v}} = (n+2j)\frac{\pi}{2} \quad , \quad j = 0, \pm 1, \pm 2, \dots \quad (43)$$

The smallest non-zero values of u for which dynamical localization is predicted by these formulae are $u_1 = 3.38$ and $u_2 = 6.77$, while we find $u_1 = 3.37$ and $u_2 = 6.75$ numerically. Figure 4 shows the time evolution of the position expectation value for $u_1 = 3.37$ (left) and for $u_3 = 5$ (right), each for $\kappa_0 = -\pi/2$. Clearly the wave packet stays and rest and does not show any systematic dispersion for $u_1 = 3.37$. Transport is found for $u_3 = 5$, where the mean transport is given by γt . However, transport is much slower than for $n = 1$ as illustrated in figure 2.

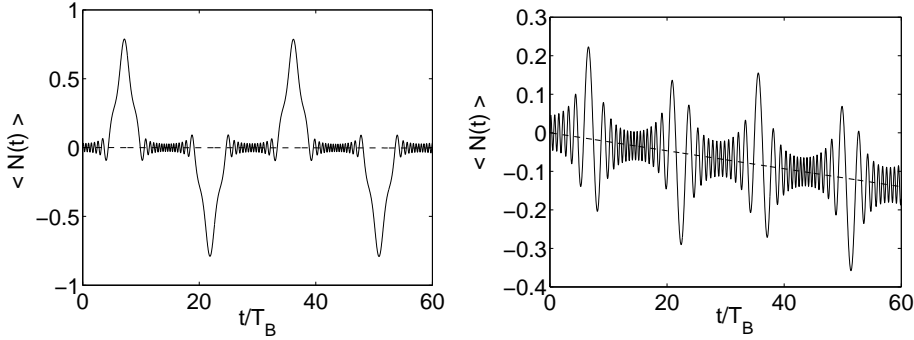


Figure 4: Dynamical Localization for $n = 29$, $v = -20$ and $u = 3.37$ (left) and transport for $u = 5$ (right). The mean transport is given by γt , which is plotted as dashed line for comparison.

5 Polychromatic driving

In view of the rich transport and localization behavior for bichromatic driving, one may expect additional surprising effects for general time periodic, however polychromatic driving. This is indeed the case, however, only few such studies have been reported up to now in particular for a periodic rectangular force [2, 14]. This case allowing a closed form solution, is discussed in the following section. The general case is briefly outlined in sect. 5.2.

5.1 Flipped fields and shuttling transport

Let us consider a rectangular force term

$$f(t) = \begin{cases} f_1 & 0 \leq t < aT \\ f_2 & aT \leq t < T \end{cases} \quad (44)$$

with $0 < a < 1$ and $f(t+T) = f(t)$. For this flipped static force excitation the time-averaged field is

$$f_0 = af_1 + bf_2 \quad , \quad b = 1 - a , \quad (45)$$

where we can assume $f_1 > 0$. For the choice $f_2 = -f_1$, the force (44) reduces to the case studied in [14] (note that there the time scale is shifted). The even more specialized case $a = 1/2$ with period $T = 2\pi/f_1$, the Bloch period for a constant field f_1 , is discussed in [15] and briefly at the end of [2] (note that in this case we have $f_0 = 0$).

For the flipped field excitation (44), the functions η_t and χ_t in (11) can be calculated by elementary integration:

$$\eta_t = \begin{cases} f_1 t & 0 \leq t \leq aT \\ f_1 aT + f_2(t - aT) & aT \leq t \leq T \end{cases} \quad (46)$$

$$\eta_{t+T} = \eta_t + \eta_T \quad , \quad \eta_T = f_1 aT + f_2 bT = f_0 t . \quad (47)$$

$$\chi_t = \begin{cases} \frac{g}{if_1} \left(1 - e^{-if_1 t} \right) & 0 \leq t \leq aT \\ \frac{g}{if_1} \left(1 - e^{-if_1 aT} \right) + \frac{ge^{-if_1 aT}}{if_2} \left(1 - e^{-if_2(t-aT)} \right) & aT \leq t \leq T \end{cases} \quad (48)$$

and

$$\chi_{t+T} = e^{-i\eta_T} \chi_t + \chi_T \quad (49)$$

$$\chi_T = \frac{g}{if_1} \left(1 - e^{-if_1 aT} \right) + \frac{g}{if_2} \left(e^{-if_1 aT} - e^{-if_0 T} \right) . \quad (50)$$

With $f_0 = \omega_B$ and $\omega = 2\pi/T$, we see that for the case of resonant driving, $\omega_B = n\omega$, we have $f_0 T = 2\pi n$, $\chi_{kT} = k\chi_T$ for $k = 1, 2, \dots$. This implies an overall transport of the expectation value $\langle \hat{N} \rangle_t$ with a velocity determined by

$$\gamma = \frac{2\chi_T}{T} = \frac{4g}{T} \left(\frac{1}{f_1} - \frac{1}{f_2} \right) e^{-i\frac{af_1 T}{2}} \sin \frac{af_1 T}{2} . \quad (51)$$

For $af_1 T = 2\mu\pi$ with $\mu = 1, 2, \dots$ we have $\gamma = 0$, i.e. dynamical localization. The maximum transport velocity

$$v_{\text{trans}} = |\gamma| = \left| \frac{4g}{T} \left(\frac{1}{f_1} - \frac{1}{f_2} \right) \sin \frac{af_1 T}{2} \right| \leq 2|g| \quad (52)$$

is obtained when the phase is adjusted as $\kappa d + \arg(\gamma) = \kappa d - af_1 T/2 = (2\mu + 1)\pi/2$ according to (23).

These findings can be easily explained in terms of Bloch oscillations for the time intervals with constant force f_1 and f_2 with Bloch periods $T_{B1} = 2\pi/f_1$ and $T_{B2} = 2\pi/|f_2|$, respectively. If $af_1 T = 2\mu\pi$ with $\mu \in \mathbb{N}$, we have $b|f_2|T = 2\nu\pi$ with $\nu \in \mathbb{N}$ for resonant driving, $f_0 = af_1 T + bf_2 T = 2n\pi$. The wave packet carries out μ full Bloch oscillations in the first time interval and ν in the second and there is no directed transport. For $af_1 T = (2\mu + 1)\pi$, however, we also have $a|f_2|T = (2\nu + 1)\pi$ ($\mu, \nu \in \mathbb{N}$) and therefore a motion

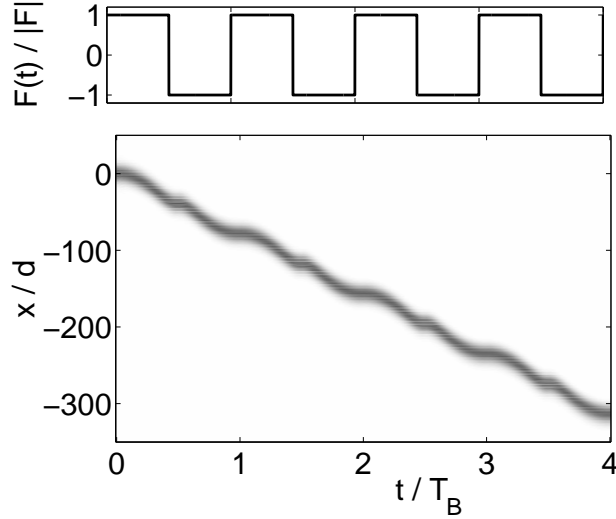


Figure 5: Numerical time propagation of a Gaussian wave packet in a cos-potential for a flipped field $f_1 = -f_2 = 0.0003$ and $a = 0.5$.

over a distance $L_1 = \Delta/F_1 = 4gd/f_1$ in the first time interval aT and $L_2 = \Delta/F_2 = 4gd/f_2$ in second time interval bT , however in the opposite direction. The average transport velocity is

$$V_{\text{trans}} = \frac{L_1 + L_2}{T} = \frac{4gd}{T} \left| \frac{1}{f_1} - \frac{1}{f_2} \right| \quad (53)$$

in agreement with (52).

Let us briefly consider the most simple case where a static field f with Bloch period $T_B = 2\pi/f$ is flipped after each half of a Bloch period, i.e. we have $f_1 = -f_2 = f$, $a = 1/2$, $f_0 = 0$ and a period $T = T_B$. This yields a transport velocity

$$v_{\text{trans}} = \frac{4|g|}{\pi}, \quad (54)$$

which is by a factor of $2/\pi$ smaller than the maximum possible value $2|g|$. It is remarkable that the velocity of this field induced transport is *independent* of the field amplitude f .

The analysis above is based on a tight-binding model, Numerically exact wave packet propagation can be used to check the validity of these predictions for realistic potentials. As an illustrating example, figs. 5 and 6 show the propagation of an initially broad Gaussian wave packet in position space,

$$\psi(x, t = 0) \sim \exp(-x^2/(2s)^2), \quad s = 15\pi \quad (55)$$

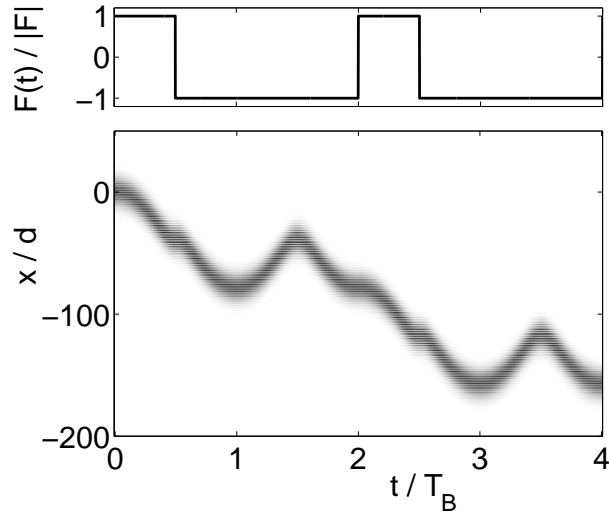


Figure 6: Numerical time propagation of a Gaussian wave packet for a flipped field $f_1 = -f_2 = 0.0003$ and $a = 1/4$.

(we use units with $\hbar = 1$) in a potential $V(x) = (1/8) \cos x$ for a flipped $F(t)$ field with $|F| = 0.0003$ and $f_1 = -f_2$. In the first case shown in fig. 5 the static force is flipped after each half-period of the Bloch time ($a = 1/2$), i.e. the average field f_0 vanishes (see also [2] for a similar calculation). One observes that the wave packet moves almost dispersionless with a velocity $V_{\text{trans}} = -78 d/T_B$, which agrees with the prediction of the tight-binding model for the actual bandwidth $\Delta = 0.0741$. Note that the direction of transport is determined by the direction of the Bloch oscillation at time $t = 0$, i.e. in the negative direction in the present case with initially positive f . In order to demonstrate this clearly, fig. 6 shows the same system as before, however for a doubled excitation period T and $a = 1/4$, i.e. a negative average force f_0 . The wave packet moves in the same direction as before, i.e. opposite to the average gradient of the potential. Note that the transport velocity is reduced by a factor of 2, because of the increased value of T . This behavior can be easily understood by observing that in the second half of the excitation period, the system undergoes a full Bloch oscillation without a net transport.

5.2 General polychromatic driving

The two simple cases analyzed above, mono- or bichromatic fields or binary-flipped piecewise constant fields allow a quite extensive analytical analysis. Let us finally briefly address a general polychromatic driving field following

[9]. For simplicity we will assume $f(t) = f(t + T)$ to be symmetric in time, $f(-t) = f(t)$, with Fourier expansion

$$f_t = f_0 - \sum_{m=1}^{\infty} f_m \cos(m\omega t) , \quad \omega = 2\pi/T . \quad (56)$$

Let us recall that in the units chosen here the dc-component is equal to the Bloch frequency $f_0 = \omega_B$, and the function η_t in eq. (11) is

$$\eta_t = \omega_B t - \sum_{m=1}^{\infty} \beta_m \sin(m\omega t) , \quad \beta_m = f_m/m\omega . \quad (57)$$

This yields

$$\begin{aligned} \chi_t &= g \int_0^t e^{-i\eta_\tau} d\tau = g \int_0^t e^{-i\omega_B \tau + i \sum_{m=1}^{\infty} \beta_m \sin(m\omega \tau)} d\tau \\ &= g \sum_{\nu=-\infty}^{+\infty} J_\nu(\{\beta_m\}) \int_0^t e^{-i(\omega_B - \nu\omega)\tau} d\tau \end{aligned} \quad (58)$$

in terms of the infinite-variable Bessel functions [16, 17]

$$\exp\left(i \sum_{m=1}^{\infty} \beta_m \sin mu\right) = \sum_{\nu=-\infty}^{+\infty} J_\nu(\{\beta_m\}) e^{-i\nu u} . \quad (59)$$

For resonant driving, $\omega_B = n\omega$, the final result is

$$\chi_t = g J_n(\{\beta_m\}) t + 2g \sum_{\nu \neq n} J_\nu(\{\beta_m\}) \frac{1}{\omega_\nu} e^{-i\omega_\nu t/2} \sin \frac{\omega_\nu t}{2} , \quad (60)$$

where we have set $\omega_\nu = \omega_B - \nu\omega$. In the non-resonant case the first term is absent and the sum extends over all integers. Specializing again to mono- or bichromatic driving this result reduces to the ones derived in sect. 3.

For resonant driving, $\omega_B = n\omega$, we have $\omega_\nu = (n - \nu)\omega$ and the oscillating part in (60) vanishes at times which are integer multiples of the driving period T . The average transport velocity is then given by

$$v_{\text{trans}} = |\gamma| = \frac{2|\chi_T|}{T} = |g J_n(\{\beta_m\})| . \quad (61)$$

Dynamical localization effects will be observed if the system parameters are tuned to a zero of the infinite-order Bessel function $J_n(\{\beta_m\})$.

The closed form result for the transport velocity in (61) is a generalization of the formula (39) derived for bichromatic driving. For the very special case of a flipped rectangular field, the closed form solution presented in section 5.1 is, of course, superior to the general solution.

6 Concluding remarks

We have shown, that the dynamics of a quantum particle in a one-dimensional periodic potential (lattice) under the action of a static and time-periodic field shows quite intricate transport and localization phenomena, even in the relatively simple case of bichromatic driving which depends sensitively on the communicability relations between the two excitation frequencies and the Bloch frequency. The theoretical analysis based on a nearest-neighbor tight-binding model allows a convenient closed form description of the transport properties in terms of generalized Bessel functions. In particular, conditions for the system parameters leading to localization are derived.

The case of polychromatic driving is also discussed, in particular for flipped static fields, i.e. rectangular pulses, which can support an almost dispersionless transport with a velocity independent of the field amplitude.

Such fields, which can be quite easily realized experimentally, offer interesting possibilities for the control of quantum transport and the manipulation of wave packets as for instance cold atoms in optical lattices.

Finally it should be noted that it offers also some advantage to modify the spatial period of the lattice. For example, a double periodic lattice, a superposition of two periodic structures with period d and $2d$ has been studied recently [18, 19]. It allows controlled Landau-Zener tunneling which can also be employed for a manipulation of matter waves.

Acknowledgments

Support from the Deutsche Forschungsgemeinschaft via the Graduiertenkolleg “Nichtlineare Optik und Ultrakurzzeitphysik” as well as from the “Studienstiftung des deutschen Volkes” is gratefully acknowledged.

References

- [1] M. Grifoni and P. Hänggi, Phys. Rep. **304** (1998) 229
- [2] T. Hartmann, F. Keck, H. J. Korsch, and S. Mossmann, New J. Phys. **6** (2004) 2
- [3] M. Glück, A. R. Kolovsky, and H. J. Korsch, Phys. Rep. **366** (2002) 103
- [4] D. H. Dunlap and V. M. Kenkre, Phys. Rev. B **34** (1986) 3625
- [5] M. Holthaus and D. W. Hone, Phil. Mag. B **74** (1996) 105

- [6] R.-B. Liu and B.-F. Zhu, *Europhys. Lett.* **50** (2000) 526
- [7] D. Suqing, Z.-G. Wang, B.-Y. Wu, and X.-G. Zhao, *Phys. Lett. A* **320** (2003) 63
- [8] K. Yashima, H. Hino, and N. Toshima, *Phys. Rev. B* **68** (2003) 235325
- [9] H. J. Korsch and S. Mossmann, *Phys. Lett. A* **317** (2003) 54
- [10] S. Mossmann, A. Schulze, D. Witthaut, and H. J. Korsch, *J. Phys. A* **38** (2005) 3381
- [11] J.-M. Lévy-Leblond, *Math. Intelligencer* **27(2)** (2005) 4
- [12] L. J. Mordell, *Diophantine Equations*, Academic Press, London and New York, 1969
- [13] H. J. Korsch, A. Klumpp, and D. Witthaut, quant-ph/0608216
- [14] M.J. Zhu, X.G. Zhao, and Q. Niu, *J. Phys.: Condens. Matter* **11** (1999) 4527
- [15] G. Lenz, R. Parker, M. C. Wanke, and C.. M. de Sterke, *Opt. Comm.* **218** (2003) 87
- [16] S. Lorenzutta, G. Maino, G. Dattoli, A. Torre, and C. Chiccoli, *Rendiconti di Matematica, Serie VII* **15** (1995) 405
- [17] F. Keck and H. J. Korsch, *J. Phys. A* **35** (2002) L105
- [18] B. M. Breid, D. Witthaut, and H. J. Korsch, *New J. Phys.* **8** (2006) 110
- [19] B. M. Breid, D. Witthaut, and H. J. Korsch, quant-ph/0607064